



**HAL**  
open science

## Wetting assessment using the dispensed drop method in the field of hot-dip galvanizing

Marie-Laurence Giorgi, Alexey Koltsov

► **To cite this version:**

Marie-Laurence Giorgi, Alexey Koltsov. Wetting assessment using the dispensed drop method in the field of hot-dip galvanizing. Galvatech 2017, Nov 2017, Tokyo, Japan. hal-01810788

**HAL Id: hal-01810788**

**<https://hal.science/hal-01810788>**

Submitted on 8 Jun 2018

**HAL** is a multi-disciplinary open access archive for the deposit and dissemination of scientific research documents, whether they are published or not. The documents may come from teaching and research institutions in France or abroad, or from public or private research centers.

L'archive ouverte pluridisciplinaire **HAL**, est destinée au dépôt et à la diffusion de documents scientifiques de niveau recherche, publiés ou non, émanant des établissements d'enseignement et de recherche français ou étrangers, des laboratoires publics ou privés.

# WETTING ASSESSMENT USING THE DISPENSED DROP METHOD IN THE FIELD OF HOT-DIP GALVANIZING

Marie-Laurence Giorgi <sup>1</sup>, Alexey Koltsov <sup>2</sup>

<sup>1</sup> CentraleSupélec, Université Paris-Saclay, Laboratoire de Génie des Procédés et Matériaux (LGPM),  
3 rue Joliot-Curie, F-91192 Gif-sur-Yvette cedex, France

<sup>2</sup> ArcelorMittal Global R&D - Maizières Process Research Centre, Voie Romaine, 57283 Maizières-lès-Metz

## ABSTRACT

In hot-dip galvanizing, the steel strip is annealed in an atmosphere of N<sub>2</sub> and H<sub>2</sub>, containing only traces of water. One of the main purposes of this heat treatment is to reduce the iron oxides present at the steel surface, in order to improve the wettability by liquid zinc. At the same time, the less-noble alloying elements (Mn, Si, P, Cr, Al) of the steel segregate to the surface and preferentially oxidize. The steel surface is then composed of metallic iron (wetted by liquid zinc) and oxide particles or films (non-wetted by liquid zinc).

The main features of wetting are first presented (surface energy, triple line, contact angle) together with simple models to estimate the equilibrium contact angle (Young's, Wenzel's and Cassie's models). Two examples of studies performed by means of the dispensed drop technique in the field of hot-dip galvanizing will then be presented: the forced wetting of a partly oxidized steel by liquid Zn - Al and the final contact angle of a liquid Zn - Al droplet on iron / silica heterogeneous surfaces.

Keyword: Selective oxidation, heterogeneous wetting, kinetic and surface energies

## INTRODUCTION

*Wetting* refers to the study of how a liquid deposited on a solid (or liquid) substrate spreads out. To begin with, the main features of wetting will be defined, namely the surface energy, the triple line, the static and dynamic contact angles and the contact angle hysteresis. Then, it will be shown how to predict the equilibrium contact angle in the case of ideal surfaces (Young's equation) and rough or heterogeneous surfaces (Wenzel's and Cassie's equations).

*Wetting* can be studied at the laboratory scale by means of the *dispensed drop technique*, in which a liquid droplet is released on a solid sample and its spreading is filmed using a high-speed camera. The parameters characteristic of the wetting can be determined from the images of the film, e.g. the impact velocity of the droplet on the solid substrate, the spreading diameter, the left and right contact angles, the contact angle hysteresis. The dispensed drop technique is particularly well suited to investigate the wettability by liquid metals. This technique will be described in the second part of the paper.

In *hot-dip galvanizing*, the wetting of the steel substrate by the liquid metal bath is the first critical step. Before immersion in the molten metal bath, the steel strip is annealed at about 800 °C in a mixture of N<sub>2</sub> and H<sub>2</sub> (5 to 15 vol.%) containing a low water partial pressure (20 to 50 Pa). This annealing allows to recrystallize the structure of the steel after cold rolling and to prevent the iron oxidation of the steel surface. However, the conditions used favour the segregation towards the surface and the oxidation of the strengthening alloying elements in steel (Si, Al and Mn for example). After annealing, the steel surface is then composed of metallic iron (wetted by liquid zinc) and oxide particles or films (non-wetted by liquid zinc). In this context, two examples of studies performed by means of the dispensed drop technique will be presented: 1) the forced wetting of a partly oxidized steel by a liquid Zn - Al droplet as a function of its initial kinetic energy and 2) the final contact angle of a liquid Zn - Al droplet obtained on heterogeneous surfaces composed of silica and iron as a function of the surface area fraction covered by silica.

## SOME FUNDAMENTALS EQUATIONS OF WETTING <sup>1-3)</sup>

*Wetting* refers to the study of how a liquid deposited on a solid (or liquid) substrate spreads out. To begin with, the main features of wetting will be defined, namely the surface energy, the triple line, the static and dynamic contact angles and the contact angle hysteresis. Then, it will be shown how to predict the equilibrium contact angle in the case of ideal surfaces (Young's equation) and rough or heterogeneous surfaces (Wenzel's and Cassie's equations).

### Definitions (surface or interfacial tension, triple line, contact angle)

The increase  $dA$  in the surface of a liquid  $L$  in contact with a vapour  $V$  requires  $\delta W$  work so that:

$$\delta W = \gamma_{LV} \cdot dA \quad (1)$$

The surface (or interfacial) tension  $\gamma_{LV}$  of liquid  $L$  in contact with vapour  $V$  is then defined as the work by surface unit (in mJ.m<sup>-2</sup>) required to increase the area of the liquid. For pure liquid zinc, at a temperature  $T$  in the range [420, 600°C] <sup>4)</sup>,

$$\gamma_{LV}[\text{mJ m}^{-2}] = (817 \pm 15) - (0.23 \pm 0.03) \cdot (T[^\circ\text{C}] - 420) \quad (2)$$

and, in particular, at 450°C,  $\gamma_{LV} = 810 \pm 16 \text{ mJ m}^{-2}$ .

Surface energies for solid / vapour and solid / liquid interfaces, called interfacial tensions and noted  $\gamma_{SV}$  and  $\gamma_{SL}$  respectively, are defined in the same way. To our knowledge, the surface energies required in the field of hot-dip galvanizing, namely  $\alpha$ -iron in equilibrium with saturated zinc vapour and  $\alpha$ -iron in contact with liquid zinc, have not been measured yet.

As a consequence of Eq. (1), in order to minimize the system's energy, a droplet placed on a solid takes the shape of a spherical cap if it is small enough in size for gravity to have negligible effect (Figure 1a). The rim of the droplet where the three phases (liquid, solid and vapour) are in contact is called the triple line. The wetting or contact angle  $\theta$  is defined by the tangent to the droplet and the horizontal substrate. The term of perfect wetting is used if  $\theta = 0^\circ$ , high partial wetting if  $\theta < 90^\circ$ , low partial wetting if  $\theta > 90^\circ$  and no wetting if  $\theta = 180^\circ$ . When the droplet is spreading on the solid, the contact angle depends on time and is called dynamic contact angle.

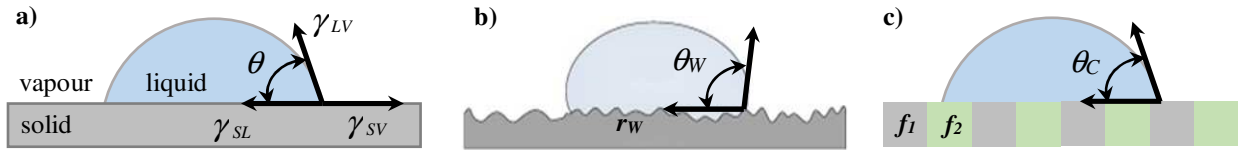


Figure 1: A small droplet in equilibrium on a) a flat horizontal surface (Young contact angle  $\theta = \theta_Y$ ), b) a rough surface (Wenzel contact angle  $\theta = \theta_W$ ) and c) an heterogeneous surface (Cassie contact angle  $\theta = \theta_C$ ).

### Equilibrium, advancing and receding contact angles

The contact angle at equilibrium on an ideal surface (i.e., smooth and homogeneous),  $\theta_Y$ , is called the Young contact angle.  $\theta_Y$  is constant at every point of the triple line and is given by Young's equation:

$$\cos \theta_Y = \frac{\gamma_{SV} - \gamma_{SL}}{\gamma_{LV}} \quad (3)$$

For non-ideal solids (i.e. rough and / or chemically heterogeneous), the contact angle  $\theta$  is not unique but lies between a receding contact angle  $\theta_r$  and an advancing contact angle  $\theta_a$ . This is called the contact angle hysteresis.

### Wenzel's and Cassie's equation

As mentioned earlier, the Young's equation is only valid for a smooth and chemically homogeneous surface. Wenzel<sup>5)</sup> and Cassie<sup>6)</sup> were among the first ones to be interested in the equilibrium contact angle obtained on rough and heterogeneous surfaces (Figures 1b and 1c).

On a randomly rough substrate (Figure 1b), the apparent contact angle at the macroscopic scale  $\theta_W$  is given by Wenzel's law. Let us consider an infinitesimal displacement  $dx$  of the triple contact line on the homogeneous rough surface. The change in the Helmholtz free energy  $dF_W$  associated with this infinitesimal displacement per unit length of the triple contact line is given by:

$$dF_W = (\gamma_{SL} - \gamma_{SV})r_W dx + \gamma_{LV} \cos \theta_W dx \quad (4)$$

Assuming that the local contact angle corresponds to the Young contact angle (Eq. 3), the macroscopic contact angle  $\theta_W$  can be given by Wenzel's law at equilibrium ( $dF_W = 0$ ):

$$\cos \theta_W = r_W \times \cos \theta_Y \quad (5)$$

with  $r_W$  the surface roughness, also called Wenzel's roughness, defined by the ratio between the actual surface area and its apparent value obtained by the horizontal plane ( $r_W \geq 1$ ).

Let us now consider the case of a smooth and randomly heterogeneous surface (Figure 1c), consisting of two different solids 1 and 2, with Young contact angles  $\theta_{Y1}$  and  $\theta_{Y2}$  and surface area fractions  $f_1$  and  $f_2 = 1 - f_1$ . An infinitesimal displacement  $dx$  of the triple contact line on the surface causes a change in the Helmholtz free energy  $dF_C$  per unit length of the triple contact line:

$$dF_C = (\gamma_{SL1} - \gamma_{SV1}) f_1 dx + (\gamma_{SL2} - \gamma_{SV2}) f_2 dx + \gamma_{LV} \cos \theta_C dx \quad (6)$$

where  $\gamma_{SLi}$  and  $\gamma_{SVi}$  are the surface energies for the solid / liquid and solid / vapour interfaces of solid  $i$  ( $i = 1$  or  $2$ ). At equilibrium, the apparent contact angle is given by Cassie's law:

$$\cos \theta_C = f_1 \cos \theta_{Y1} + f_2 \cos \theta_{Y2} \quad (7)$$

### METHODS OF MEASURING WETTABILITY PARAMETERS

At high temperature, *wetting* can be studied by means of the sessile drop method or the wetting balance technique. There are several variants of the sessile drop method: classic technique, in-situ formation of a liquid alloy, dispensed drop, transferred drop, double substrate and tilted plate<sup>7)</sup>.

The *dispensed drop technique* is particularly well suited to study the wettability by liquid metals. With this technique, a liquid droplet is released on a solid sample (Figure 2) and its spreading is filmed using a high-speed camera (Figure 3). The parameters characteristic of wetting can be determined from the images of the film. The impact velocity  $V_0$  of the droplet on the solid substrate is given by:

$$V_0 = V_m + \frac{1}{2} g t_{drop} \quad (8)$$

where  $V_m$  is the average velocity, i.e. the ratio of the displacement  $h$  of the droplet (from the capillary exit to the substrate) to the time  $t_{drop}$  it had taken to cover that displacement (Figures 2a and 2d) and  $g$  is the gravitational acceleration. The initial kinetic energy of the droplet is therefore given by:

$$E_{K0} = \frac{1}{2} m V_0^2 \quad (9)$$

The spreading diameter and the left and right contact angles can be measured as a function of spreading time as shown in Figure 3 ( $t = 1000$  ms). The contact angle hysteresis can also be determined when the drop advances and reaches a maximal spreading diameter before receding. The spreading rate of the triple line is then zero for a few ms, which makes it possible to measure the advancing and receding contact angles. This is the case when the initial kinetic energy of the drop is high enough.

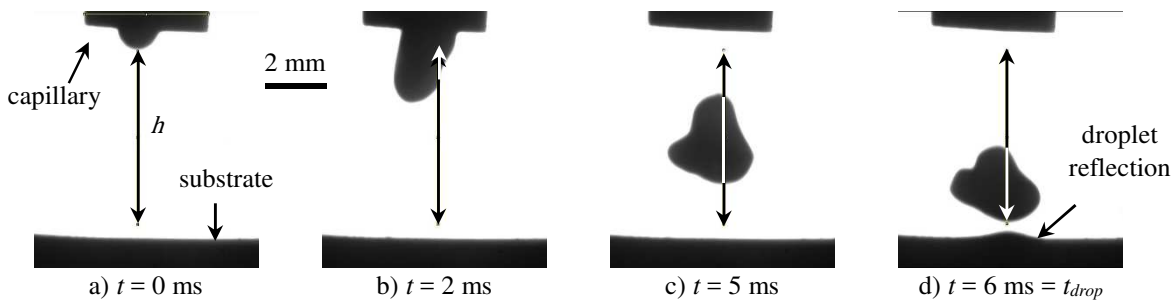


Figure 2: Dispersed drop technique in which the liquid metal droplet is extruded from an alumina capillary (a and b) and released on a solid substrate (c and d). This image sequence is used to estimate the impact velocity of the drop on the solid ( $h$  is the distance travelled by the drop between the capillary and the substrate).

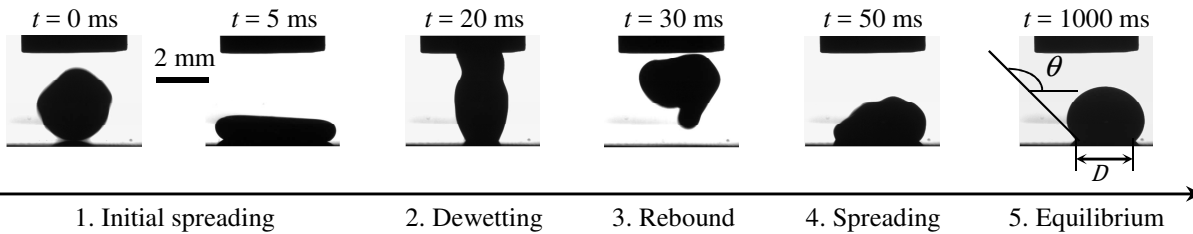


Figure 3: Spreading of a liquid lead droplet on  $\text{SiO}_2$  at  $450^\circ\text{C}$ . The initial spreading is followed by a dewetting and a rebound of the liquid metal droplet.

In *hot-dip galvanizing*, the wetting of the steel substrate by liquid zinc is the necessary condition to ensure the adhesion and homogeneity of zinc coating. As it was already mentioned in the Introduction section, before immersion in the liquid metal bath, steel undergoes an annealing treatment at about  $800^\circ\text{C}$  in a reducing atmosphere  $\text{N}_2\text{-H}_2$  (5 to 15 vol.%) containing traces of water (about  $-30^\circ\text{C}$  frost point). During this treatment, the iron oxides are reduced and the less-noble alloying elements of the steel (e.g., Si, Mn, Al) segregate to the steel surface where they form oxide particles or films that are poorly wetted by liquid zinc<sup>8,9</sup>. Several studies have investigated the influence of steel oxidation on wettability by liquid zinc<sup>10-17</sup>. In these experimental studies, the wettability by liquid zinc alloys of heterogeneous surfaces composed of metallic iron and oxides was investigated at approximately  $460^\circ\text{C}$  by means of the wetting balance technique<sup>10,11</sup> or the dispensed drop method<sup>12-17</sup>. It was shown that wettability is deteriorated (i.e., higher contact angle, slower wetting rate) if the surface area fraction covered by oxides is increased.

Two examples of studies performed by means of the dispensed drop technique in the field of hot-dip galvanizing will be presented below: 1) the forced wetting of a partly oxidized steel by liquid Zn - Al and 2) the influence of the surface area fraction covered by silica (for heterogeneous surfaces composed of silica and iron) on the final contact angle of a liquid Zn - Al droplet at short contact time.

## FORCED WETTING OF A PARTLY OXIDIZED STEEL BY LIQUID ZN - AL

The forced wetting of a partly oxidized steel by liquid Zn - Al was investigated by means of the dispensed drop technique. The spreading of the liquid metal droplet as a function of its initial kinetic energy was observed and filmed.

### Brief description of the dispensed drop experiments

The experimental system is described in details elsewhere<sup>18)</sup>. The solid substrate is first heated to  $850 \pm 2^\circ\text{C}$  in 1 hour in an atmosphere of  $\text{N}_2$ -5 vol.%  $\text{H}_2$  with a frost point equal to  $-45^\circ\text{C}$ . It is then cooled down to  $452 \pm 4^\circ\text{C}$  and maintained at this temperature. The liquid metal droplet is then released on the solid substrate at the same temperature. For these trials, the impact velocity  $V_0$  of the droplet on the solid substrate was increased from 0.6 to  $1.5 \text{ m s}^{-1}$ . The spreading of the liquid metal droplet on the solid sample is filmed by means of a high-speed camera (*pco.1200hs*) with a recording speed of 1000 images per second and a  $780 \times 501$  pixel resolution. During the wettability experiments, the frost point in the furnace chamber is equal to  $-54 \pm 3^\circ\text{C}$  (i.e., partial pressure of water of 1.6 - 3.5 Pa). This frost point corresponds to a partial pressure of oxygen in the range of  $3.10^{-32}$ - $7.10^{-33}$  Pa at  $450^\circ\text{C}$  (assuming that the thermodynamic equilibrium is reached). An image analysis procedure is performed to obtain the experimental contour of the droplet. Contact angles and spreading diameters are calculated by means of the *Drop Snake Approach*<sup>19)</sup> with ImageJ software<sup>20)</sup>. The error of the contact angle has been estimated to be less than  $\pm 5^\circ$ .

### Materials

The wettability experiments were performed on a cold-rolled Interstitial Free Titanium (*IF Ti*) ferritic steel (*ArcelorMittal*). Its composition is listed in Table 1. Before the experiments, the substrates were polished up to  $1 \mu\text{m}$ . The average surface roughness  $R_a$  obtained was less than 2 nm.

Table 1: Average composition of the *IF Ti* steel studied (wt.%)

C	Si	Mn	P	Al	Cr	Ti	B	S	N	V	As	Cu	Ni	Sn
0.002	0.009	0.117	0.013	0.027	0.017	0.074	0.0001	0.008	0.005	0.002	0.002	0.018	0.023	0.004

During the annealing treatment described before, the steel substrate became covered with tiny particles (Figures 4a and 4b). Mn, Al, Si and O were detected in these particles by Energy Dispersive Spectroscopy (EDS *Princeton Gamma-Tech* in a Field Emission Gun Scanning Electron Microscope FEG-SEM *LEO 1530*). Thermodynamic calculations show that iron oxides are completely reduced under the annealing conditions chosen and Mn, Al and Si are oxidized<sup>21)</sup>. The surface studied will then be metallic iron partly covered with oxide particles.

The steel surface also exhibits a strong faceting, varying from one grain to the other. The average roughness  $R_a$  and maximum roughness  $R_t$  were measured by Atomic Force Microscopy (AFM *Digital Instruments Nanoscope IIIA*) or 3D optical surface profiler (*ZYGO, NView 6K*):  $R_a = 9 \pm 2 \text{ nm}$  and  $R_t \sim 100 \text{ nm}$ . In all cases, the samples can be presumed to be smooth for the wettability experiments<sup>7)</sup>.

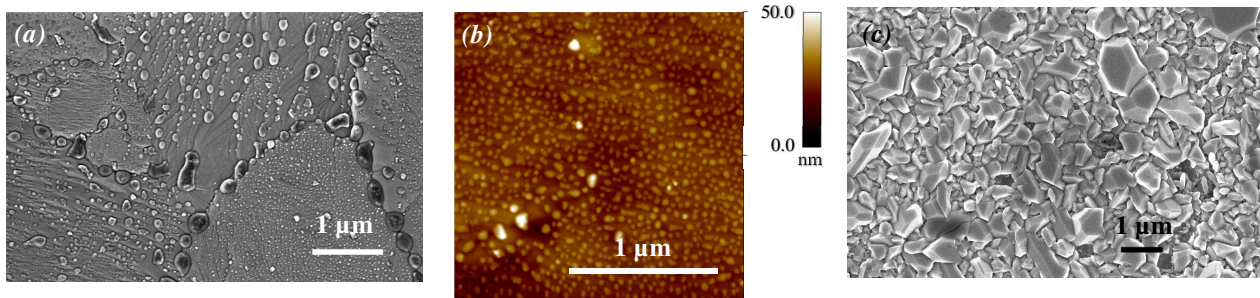


Figure 4: a) FEG-SEM and b) AFM images of the steel surface after annealing, c) FEG-SEM image of  $\text{Fe}_2\text{Al}_5\text{Zn}_x$  formed at the interface between solid metal and liquid Zn-Al (after preferential dissolution of the solidified drop).

The liquid metal droplets are produced from shots of zinc containing  $0.18 \pm 0.05 \text{ wt.}\%$  Al and  $0.010 \pm 0.010 \text{ wt.}\%$  Fe. The analysis was performed by Atomic Absorption Spectroscopy (AAS, *SpectrAA, Varian*). The liquid metal is saturated in iron (liquid phase in equilibrium with  $\text{Fe}_2\text{Al}_5\text{Zn}_x$ ). The droplet weight  $m$  is equal to  $80.0 \pm 0.2 \text{ mg}$  in all experiments. If the liquid metal droplet is supposed to be spherical before spreading, its diameter  $D_0$  is given by:

$$m = \frac{\pi}{6} D_0^3 \rho_{Liq} \quad (10)$$

where  $\rho_{Liq}$  is the liquid metal density supposed to be equal to the liquid zinc density (6525 kg.m<sup>-3</sup> at 450°C<sup>22</sup>), the Al and Fe contents being very low.

### Dynamic spreading of the liquid zinc droplet

The evolution of both the dimensionless diameter and the contact angle as a function of spreading time and initial kinetic energy of the drop are shown in Figure 5. During the first milliseconds of spreading, the contact angle remains constant at a value of about 120° and the spreading diameter increases. The contact angle then decreases sharply until it reaches its minimum value after 14 ms of spreading. Meanwhile, the spreading diameter continues to increase up to its maximum value  $D_{max}$ . Finally, after approx. 100 ms of spreading, the contact angle and spreading diameter reach their final value. As a conclusion, the final spreading diameter increases and the final contact angle decreases as the drop's initial kinetic energy increases.

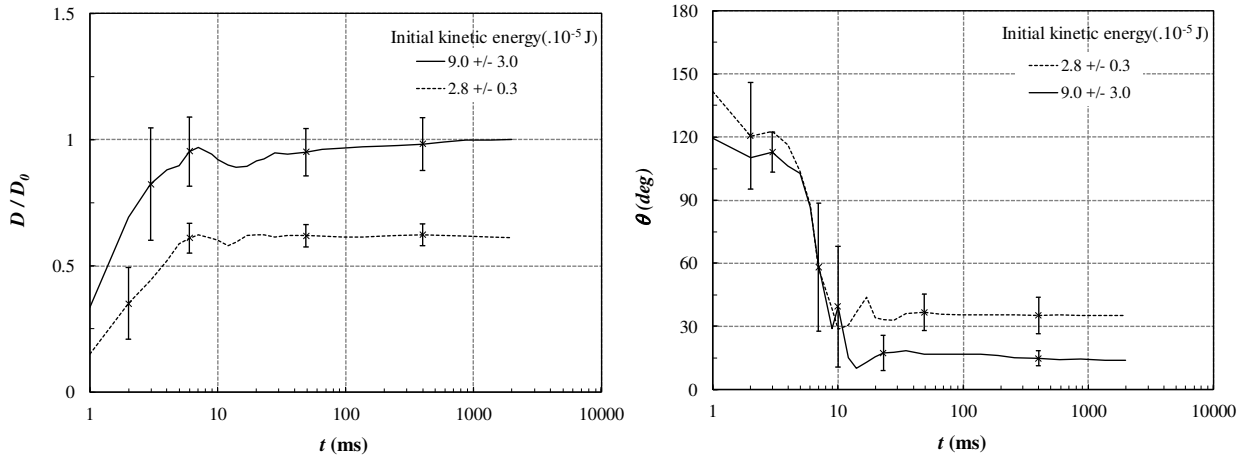


Figure 5: Effect of the initial kinetic energy of the zinc alloy droplet on the evolution of the dimensionless spreading diameter  $D/D_0$  (left) and the contact angle (right) as a function of time.

The wetting between metallic iron and liquid Zn-Al is reactive with the dissolution of iron and the nucleation and growth of  $Fe_2Al_5Zn_x$  ( $0 < x < 1$ )<sup>8,9</sup>. The preferential dissolution of the solidified droplet makes it possible to highlight the interface compound formed at the iron / Zn-Al alloy interface (Figure 4c). The surface is covered with small crystals, whose shape is characteristic of  $Fe_2Al_5Zn_x$  observed on industrial products. An EDS analysis confirms that these small crystals are rich in aluminium. The average surface roughness of this interface alloy  $R_a$  is of the order of 180 nm.

During the first stage of spreading, until the drop spreading diameter reaches its maximum value, the wetting of the liquid metal drop is forced by its initial kinetic energy. It can be assumed that the initial contact angle (which is high) corresponds to the contact angle of the liquid metal on the partly oxidized solid metal (Figures 4a and 4b) before the formation of the interface alloy. The final contact angle corresponds to the contact angle obtained on  $Fe_2Al_5Zn_x$ .

The final contact angle is unique and given by the Young contact angle for a smooth and chemically homogeneous surface (Eq. 3). In our case, the final contact angle decreases with the increasing initial kinetic energy of the drop, which means that the liquid zinc drop remains pinned in a metastable position. In fact, the interfacial reaction occurring during drop spreading blocks the receding of the droplet. Consequently, the contact angle hysteresis in this case is induced by the interfacial reactivity.

### WETTING OF IRON / SILICA SURFACES BY LIQUID ZN - AL

Wetting experiments were performed by means of the dispensed drop technique. The objective was to study the influence of the surface area fraction covered by silica on the final contact angle of liquid Zn - Al droplets on iron / silica heterogeneous surfaces at short contact time. The final contact angles obtained were compared to Cassie's law (Eq. 7). The experimental setup was described before.

### Materials

The wettability experiments were performed on iron – silicon substrates (*Goodfellow*), with a Si content in the range [0.032, 0.485] wt.% (Table 2). The principal impurities are C (< 0.0015 wt.%), Mn (< 0.003 wt.%), P (< 0.003 wt.%), S (< 0.0025 wt.%), Cr (< 0.005 wt.%), Ti (0.001 wt.%), Al (< 0.003 wt.%) and B (< 0.0017 wt.%). The experimental results

are compared with those obtained on a high purity iron substrate (99.98 wt.%, the principal impurities being Si, Mn, Cr and Ti). Before the experiments, the substrates were polished up to 1  $\mu\text{m}$ . The average surface roughness  $R_a$  obtained was less than 8 nm.

During the annealing treatment described before, the iron – silicon substrates became covered with tiny particles ( $FeSi0.03$ ,  $FeSi0.06$ ,  $FeSi0.08$ ,  $FeSi0.1$ ,  $FeSi0.15$ ) or films ( $FeSi0.25$ ,  $FeSi0.5$ ) (Table 2, Figures 6b and 6c). Si was detected in these particles and films by Energy Dispersive Spectroscopy (EDS *Princeton Gamma-Tech* in a Field Emission Gun Scanning Electron Microscope FEG-SEM *LEO 1530*). The *Iron* surface exhibits a strong faceting, varying from one grain to the other, and a thermal grooving of grain boundaries. A few rare globular shaped particles can be observed (Figure 6a).

Thermodynamic calculations show that iron oxides are completely reduced under the annealing conditions chosen and silicon is oxidized into  $SiO_2$ <sup>21</sup>). The surfaces studied will then be pure metallic iron for the *Iron* samples and metallic iron partly or completely covered with  $SiO_2$  particles or films for the iron-silicon substrates. An image analysis procedure is used to estimate the percentage in surface area covered by silica  $f_{silica}$  for the Fe-Si alloys after annealing.  $f_{silica}$  varies from 0.2 to 100 %.

The average roughness  $R_a$  and maximum roughness  $R_t$ , measured by Atomic Force Microscopy (AFM *Digital Instruments Nanoscope IIIA*) or 3D optical surface profiler (*ZYGO, NView 6K*) are given in Table 2 for each sort of sample. The average roughness  $R_a$  is less than 8 nm. The grain-boundary grooves formed on *Iron* substrates (given by  $R_t$  values) do not cause any distortion of the triple line. In all cases, the samples can be presumed to be smooth for the wettability experiments<sup>7</sup>). The effect of the Wenzel's roughness (Eq. 5) will therefore be presumed to be negligible.

Table 2: Characterization of the substrates after the annealing treatment (surface area fraction covered by silica  $f_{silica}$ , average surface roughness  $R_a$ , maximum roughness  $R_t$ )

	<i>Iron</i>	$FeSi0.03$	$FeSi0.06$	$FeSi0.06$	$FeSi0.08$	$FeSi0.1$	$FeSi0.15$	$FeSi0.25$	$FeSi0.5$
Si (wt.%)	0.0002	0.032	0.057	0.061	0.077	0.097	0.150	0.245	0.485
$SiO_2$	P <sup>(a)</sup>	F <sup>(b)</sup>	F <sup>(b)</sup>						
$f_{silica}$ (%)	$0.2 \pm 0.2$	$0.4 \pm 0.2$	$23 \pm 3$	$26 \pm 2$	$34 \pm 6$	$38 \pm 8$	$43 \pm 5$	$74 \pm 10$	100
$R_a$ (nm)	$2 \pm 1$	$2 \pm 1$	$2 \pm 1$	$8 \pm 1$	$7 \pm 1$	$3 \pm 1$	$4 \pm 1$	$5 \pm 1$	$4 \pm 1$
$R_t$ (nm)	$216 \pm 42$	$143 \pm 21$	$43 \pm 6$	$80 \pm 9$	$92 \pm 8$	$175 \pm 6$	$122 \pm 6$	$128 \pm 61$	$111 \pm 44$

<sup>(a)</sup> P stands for small discrete  $SiO_2$  particles; <sup>(b)</sup> F for  $SiO_2$  films.

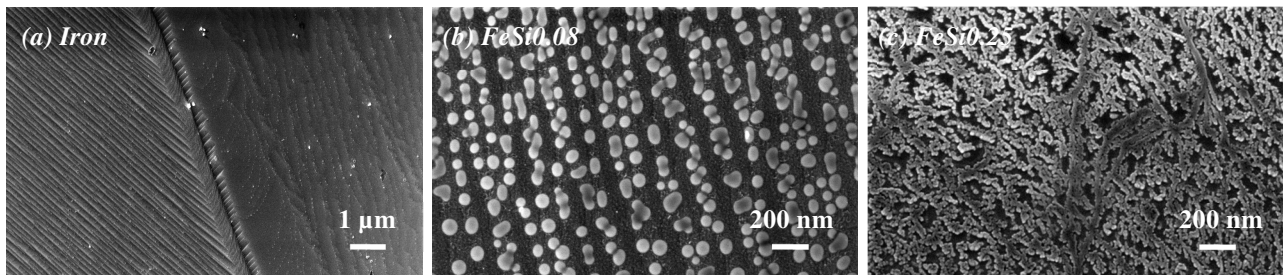


Figure 6: FEG-SEM images of the substrate surface after the annealing treatment for a) *Iron*, b)  $FeSi0.08$  and c)  $FeSi0.25$  alloys. The  $FeSi0.08$  alloy is covered with globular  $SiO_2$  particles and the  $FeSi0.25$  alloy surface is completely covered by a  $SiO_2$  film.

The liquid metal droplets are produced from shots of zinc containing  $0.18 \pm 0.05$  wt.% Al and  $0.010 \pm 0.010$  wt.% Fe. The droplet weight  $m$  is equal to  $80.0 \pm 0.2$  mg in all experiments.

### Final contact angles

This part of the study is focused on the final contact angle  $\theta_f$  reached at the end of the spreading as a function of the surface area fraction covered by silica from pure iron to pure silica (Table 2). In Figure 7, the experimental points obtained are represented by red squares and compared to the Cassie contact angle (Eq. 7) estimated in two cases:

- The drop can penetrate between the silica particles or films and be in contact with the  $Fe_2Al_5Zn_x$  formed and silica. At equilibrium, the apparent contact angle is related to the Young contact angles on  $Fe_2Al_5Zn_x$  and silica and to the Wenzel

roughness  $r_w$ . As the average roughness  $R_a$  and the maximum roughness  $R_t$  are low, the samples can be presumed to be smooth for the wettability experiments, i.e.  $r_w = 1$ . The equilibrium contact angle is then given by:

$$\cos\theta_C = (1 - f_{silica})\cos\theta_{Fe_2Al_5Zn_x} + f_{silica}\cos\theta_{silica} \quad (11)$$

where  $\theta_{Fe_2Al_5Zn_x}$  and  $\theta_{silica}$  are the Young contact angles on  $Fe_2Al_5Zn_x$  and silica respectively and  $f_{silica}$  is given in Table 2. The Cassie contact angle is represented by the blue curve in Figure 7.

• Conversely, the drop can remain in contact with an air / substrate composite surface. Assuming that the contact angle in air is  $\theta_{air} = 180^\circ$ , the apparent contact angle is then related to  $f_{silica}$  and  $\theta_{silica}$  only:

$$\cos\theta_C = -1 + f_{silica} + f_{silica}\cos\theta_{silica} \quad (12)$$

The Cassie contact angle obtained is represented by the pink curve in Figure 7.

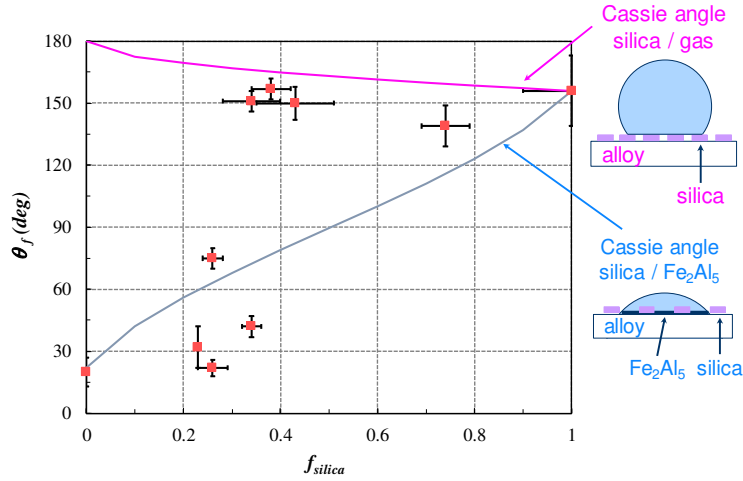


Figure 7: Final contact angles (red squares) between liquid Zn-Al and iron / silica substrates as a function of the surface area fraction covered by silica. The experimental points are compared with the Cassie contact angles estimated for the drop in contact with silica and air (pink curve) or silica and  $Fe_2Al_5Zn_x$  (blue curve)

In our experiments, pure iron is wetted by liquid Zn-Al alloy (0.2 wt.%) saturated in iron with a contact angle of about  $22^\circ$ . This contact angle is of the same order of magnitude as the measurements found in the literature for the iron / zinc system at short contact times <sup>23</sup>. Silica is not wetted by the Zn-Al alloy used. The high contact angle obtained ( $157^\circ$ ) is of the same order of magnitude as the contact angle measured for zinc on vitreous silica ( $133^\circ$  to  $500^\circ C$  <sup>24</sup>). The final contact angle increases with the surface area fraction covered by silica. This is in good agreement with previous results found in the same experimental conditions, i.e. wetting by Zn - Al (0.2 wt.%) alloy of Fe / Si substrates annealed under a  $N_2 / H_2$  atmosphere at low dew point <sup>26</sup>. The authors showed that the higher the silicon content in the alloy, the higher the final contact angle. However, they did not measure the corresponding surface area fraction of silica as we did.

The contact angles measured for the iron / silica substrate with  $f_{silica} = 34\%$  are very different from each other: among the six angles measured for this system, three are high (about  $150^\circ$ ) and three are low (about  $40^\circ$ ). It therefore seems that the transition between wetting and non-wetting corresponds to surface area fractions covered by silica of about 34% with the experimental conditions used here.

For surface area fractions covered by silica below this limit of 34%, the Fe /  $SiO_2$  substrates are wetted by the liquid metal with a contact angle lower than the Cassie contact angle estimated on  $Fe_2Al_5Zn_x / SiO_2$  substrates. The explanation might be that the initial wetting of the liquid metal drop is forced by the kinetic energy of the droplet. The droplet is then receding before reaching its final position. In our experiments, the surface defects are the oxide particles which are less wetted than metallic iron by liquid Zn - Al and represent barriers for advancing and receding liquid front. Moreover, the formation of the interfacial product ( $Fe_2Al_5Zn_x$ ) creates a complementary barrier to receding of the liquid. Thus, the final contact angle is then a receding contact angle close to the contact angle measured on the better wetted parts of the surface (here  $Fe_2Al_5Zn_x$  formed on metallic iron).

For surface area fractions covered by silica more than 34%, the final contact angle is close to the Cassie contact angle calculated on air /  $SiO_2$  substrates. This means that, in this case, bubbles are trapped in between the silica particles or films (no intimate contact between metallic iron and liquid alloy is created).

## CONCLUSION

*Wetting* refers to the study of how a liquid deposited on a solid (or liquid) substrate spreads out. To begin with, the main features of wetting were defined, namely the surface energy, the triple line, the static and dynamic contact angles and the contact angle hysteresis. Then, simple models used to predict the equilibrium contact angle in the case of ideal surfaces (Young's equation) and rough or heterogeneous surfaces (Wenzel's and Cassie's equations) were presented.

*Wetting* can be studied at the laboratory scale by means of the *dispensed drop technique*, in which a liquid droplet is released on a solid sample and its spreading is filmed using a high-speed camera. This technique was described in detail together with the parameters characteristic of the wetting which can be determined, e.g. the impact velocity of the droplet on the solid substrate, the spreading diameter, the left and right contact angles, the contact angle hysteresis.

Two examples of studies performed by means of the dispensed drop technique were presented in the field of hot-dip galvanizing:

- 1) The forced wetting of a partly oxidized steel by liquid Zn - Al was investigated. The spreading of the liquid metal droplet as a function of its initial kinetic energy was observed and filmed. The final contact angle decreases significantly when the kinetic energy of the droplet is increased. The experimental results can be related to the reactions occurring at the interface between the steel and the molten metal at very short contact time.
- 2) Wetting experiments were performed to measure the final contact angle of a liquid Zn - Al droplet as a function of the surface area fraction covered by silica (for heterogeneous surfaces composed of silica particles or films and iron) at short contact time. The spreading of the liquid metal droplet strongly depends on the surface area fraction covered by silica. The transition between wetting and non-wetting was found for surface area fractions covered by silica of about 34% with the experimental conditions used here. The final contact angles obtained were compared to Cassie's equation. This shows that, for  $f_{silica} < 34\%$ , the final contact angle is a receding contact angle on iron parts of the surface and for  $f_{silica} > 34\%$  bubbles are trapped in between silica particles or films due to a high non-wetting contact angle.

## ACKNOWLEDGEMENTS

The authors are extremely grateful to the staff of CentraleSupélec for their valuable assistance (N. Ruscasiser, A. Ollivier, J. Diawara, J. Trubuil). They extend their thanks to Jean-Michel Mataire for fruitful discussions.

## REFERENCES

- 1) P. G. de Gennes: Rev. Modern Phys., 57 (1985) 827.
- 2) D. Quéré: Rep. Prog. Phys., 68 (2005) 2495.
- 3) W. D. Kaplan, D. Chatain, P. Wynblatt, W. C. Carter: J. Mater. Sci., 48 (2013) 5681.
- 4) B. J. Keene: Int. Mater. Rev., 38 (1993) 157.
- 5) R. N. Wenzel: Ind. Eng. Chem., 28 (1936) 988.
- 6) A. B. D. Cassie, S. Baxter: Trans. Faraday Soc., 40 (1944) 546.
- 7) N. Eustathopoulos, M.G. Nicholas, B. Drevet: Wettability at High Temperatures, Pergamon Materials Series, Elsevier Science, Oxford, UK, 1999.
- 8) M. Guttman: Mat. Sci. Forum, 155/156 (1994) 527.
- 9) A. R. Marder: Prog. Mater. Sci., 45 (2000) 191.
- 10) Y. Hirose, H. Togawa, J. Sumiya: Tetsu-to-Hagané, 68 (1982) 658.
- 11) Y. Hirose, H. Togawa, J. Sumiya: Tetsu-to-Hagané, 68 (1982) 665.
- 12) S. Frenznick, S. Swaminathan, M. Stratmann, M. Rohwerder: J. Mater. Sci., 45 (2010) 2106.
- 13) J. Lee, J. Park, Y. Kim, S.-H. Jeon: J. Mater. Sci., 45 (2010) 2112.
- 14) L. Bordignon, X. Vanden Eynde: Rev. Métall., 104 (2007) 300.
- 15) T. Kawano, F. U. Renner: ISIJ Int., 51 (2011) 1703.
- 16) T. Kawano, F. U. Renner: Surf. Interface Anal., 44 (2012) 1009.
- 17) M.-L. Giorgi, J. Diawara, S. Chen, A. Koltsov, J.-M. Mataire: J. Mater. Sci., 47 (2014) 8483.
- 18) M. Zaïdi, M.-L. Giorgi, J.-B. Guillot, F. Goodwin: Mater. Sci. Eng. A, 495 (2008) 90.
- 19) A. F. Stalder, G. Kulik, D. Sage, L. Barbieri, P. Hoffmann: Colloids Surf. A, 286 (2006) 92.
- 20) W. S. Rasband: Image J, U. S. National Institutes of Health, Bethesda, Maryland, USA, (1997-2017), <http://imagej.nih.gov/ij/>.
- 21) D. Huin, P. Flauder, J.-B. Leblond: Oxid. Met., 64 (2005) 131.
- 22) L. D. Lucas: Techniques de l'ingénieur, Traité des Matériaux Métalliques, (1996), M65:1 (in French).
- 23) S.I. Popel, T.V. Zakharova, V.V. Pavlov: Fiz. Khim. Issled. Met. Protsessov, 3 (1975) 108.
- 24) J.E. Kelley, H.M. Harris: J. Test. Eval., 2 (1974) 40.
- 25) S. Frenznick, M. Stratmann, M. Rohwerder: Proc. of the 6<sup>th</sup> Int. Conf. on Zinc and Zinc Alloy Coated Sheet Steels Galvatech'04, Chicago, USA, The Association for Iron and Steel Technology, (2004) 411.